BioChip Journal
https://doi.org/10.1007/s13206-022-00064-1

REVIEW ARTICLE

Recent Developments in Innovative Magnetic Nanoparticles-Based Immunoassays: From Improvement of Conventional Immunoassays to Diagnosis of COVID-19

Yeonjeong Ha[1] · **Ijung Kim**[2]

Received: 7 March 2022 / Revised: 1 May 2022 / Accepted: 30 May 2022

Abstract
During the ongoing COVID-19 pandemic, the development of point-of-care (POC) detection with high sensitivity and rapid detection time is urgently needed to prevent transmission of infectious diseases. Magnetic nanoparticles (MNPs) have been considered attractive materials for enhancing sensitivity and reducing the detection time of conventional immunoassays due to their unique properties including magnetic behavior, high surface area, excellent stability, and easy biocompatibility. In addition, detecting target analytes through color development is necessary for user-friendly POC detection. In this review, recent advances in different types of MNPs-based immunoassays such as improvement of the conventional enzyme-linked immunosorbent assay (ELISA), immunoassays based on the peroxidase-like activity of MNPs and based on the dually labeled MNPs, filtration method, and lateral-flow immunoassay are described and we analyze the advantages and strategies of each method. Furthermore, immunoassays incorporating MNPs for COVID-19 diagnosis through color development are also introduced, demonstrating that MNPs can become common tools for on-site diagnosis.

Keywords Magnetic nanoparticles · Immunoassay · Point-of-care detection · COVID-19

1 Introduction

Due to the worldwide COVID-19 pandemic, the rapid and accurate diagnosis of diseases has become a critical factor to prevent the spread of diseases between persons and communities. Currently, reverse transcription polymerase chain reaction (RT-PCR) is the standard method for detecting severe acute respiratory syndrome coronavirus 2 (SARS-CoV-2), the virus that causes COVID-19. Although the RT-PCR has high sensitivity and reproducibility to detect the virus, it takes a long time and requires expensive instruments as well as professional labor [1]. Immunoassay-based rapid diagnosis detection kits (RDTs) for SARS-CoV-2 have been actively developed and widely used as point-of-care (POC) diagnosis; however, false-negative cases have been frequently reported for RDTs [2]. Developing rapid diagnosis detection methods with high sensitivity and specificity is thus urgently needed [3]. In addition, the development of ultrasensitive detection methods enables non-invasive and painless sampling (e.g., saliva sampling), which is particularly suitable for young children.

Recently, iron oxide magnetic nanoparticles (MNPs) have received interest as promising materials for rapid and high-sensitive diagnosis methods due to their unique properties [4]. First, MNPs act as "nano-magnets" with the presence of an external magnet. They move rapidly toward the external magnet while their magnetism is instantly lost when the magnetic field is removed [5]. Second, it is well acknowledged that MNPs are stably conjugated with various biomaterials without losing their magnetic properties. Because of these capabilities, MNPs allow magnetic pre-concentration of target materials from a very dilute concentration via two steps: (i) target materials interact with bioconjugated MNPs, and (ii) target material-bioconjugated MNPs are collected with an external magnet and re-dispersed into a small volume of matrix for the pre-concentration of samples to improve the detection sensitivity. In addition, MNPs offer

✉ Yeonjeong Ha
gbhyjyh@korea.ac.kr

[1] Division of Environmental Science and Ecological Engineering, Korea University, 145 Anam-ro, Seongbuk-gu, Seoul 02841, Republic of Korea

[2] Department of Civil and Environmental Engineering, Hongik University, 94 Wausan-ro, Mapo-gu, Seoul 04066, Republic of Korea

Published online: 05 July 2022

low background noise, since the biological molecules that do not interact with MNPs are non-magnetic [6]. Furthermore, MNPs offer high surface area, which can allow fast detection time via rapid interaction between the target materials and bioconjugated MNPs. Indeed, MNPs have been effectively applied to rapid and highly sensitive detection for a broad range of target analytes from viruses [7, 8] and bacteria [9, 10] to food allergen [11, 12]. Furthermore, it is worth noting that the latest studies have incorporated MNPs-based immunoassays with a CRISPR (clustered regularly interspaced short palindromic repeats)/Cas system, which is an attractive method for specific recognition of infectious bacteria and viruses [13, 14]. For example, Kim et al. [13] applied MNPs to a CRISPR/Cas system combined with surface-enhanced Raman scattering (SERS) assay to detect multidrug-resistant (MDR) bacteria. In the assay, MNPs achieve high sensitivity because their superparamagnetic properties provide effective separation and purification of target samples and are applicable to SERS. MNPs were also applied to a CRISPR/Cas system to detect *Salmonella typhimurium* (*S. typhimurium*) in food samples [14]. In this study, polyclonal antibody-conjugated MNPs allow for magnetic separation of target bacteria, achieving rapid and ultrasensitive detection.

Considering that these unique properties of MNPs are key advantages for immunoassays, review papers have introduced the recent development of MNP-based immunoassays and many of them mainly focused on immunoassays incorporating biosensors. These require extra instruments, such as electrochemical or fluorescent analysis, nuclear magnetic resonance (NMR), superconducting quantum interference device (SQUID), and giant magneto-resistance (GMR) [5, 15–17]. On the other hand, detecting the target material via the naked eye through color development is a user-friendly and low-cost POC detection method. Thus, this review focuses on the different types of MNP-based immunoassays for POC detection via color development and describes the fundamental theory and MNP characteristics for the application of MNPs to each type of immunoassay. Furthermore, recent developments of MNP-based immunoassay for COVID-19 diagnosis via color development are described and their strengths compared to the conventional diagnosis method are analyzed. Before describing the different types of MNPs, this review begins with a brief introduction of MNP preparation methods for immunoassay applications.

2 Preparation of MNPs for Immunoassay Applications

2.1 MNP Preparation

Most core MNPs applied in immunoassays are in iron oxide form such as magnetite (Fe_3O_4) or maghemite (γ-Fe_2O_3). Although such MNPs with various sizes, shapes, and surface functionalities are commercially available, many homemade MNP synthesis approaches have been introduced [18, 19] and MNPs conjugated with metals/inorganics as nanocomposites recently have drawn attention [20, 21]. Since MNP synthesis via chemical co-precipitation was originally reported [22], this has been widely used as a facile and convenient synthesis strategy in various applications including immunoassays (Fig. 1a) [23–26]. Thermal decomposition is preferred to synthesize the monodispersed magnetic nanoparticles of the order of nanometers (Fig. 1b) [27]. Although a high area to volume ratio is favorable for capturing target components and enhancing the sensitivity, MNP size control is desirable as MNPs could lose their superparamagnetic property as the size decreases [28, 29]. To enhance the magnetic property while keeping small MNPs, microbeads as a cluster of MNPs in a confined space have been utilized [30].

2.2 MNPs Incorporated in Biomaterials

Since MNPs in the form of iron oxide have been used as a tool for cancer treatment via hyperthermia for decades [31], many researchers have reported conjugation with a ligand of high affinity to cancer cells [32, 33]. Recently, antibodies or engineering antibodies targeting the antigens of interest have been incorporated with MNPs as a diagnostic tool [5]. In particular, the selection of an antibody as a specific receptor

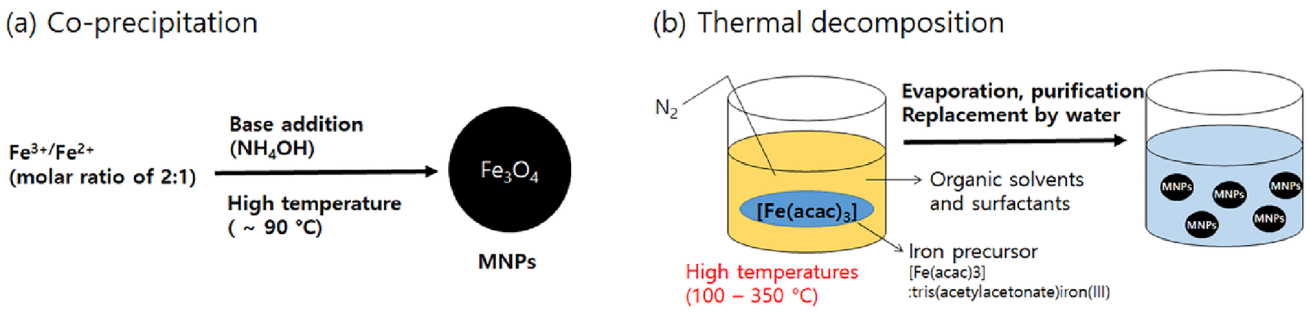

Fig. 1 Depiction of the **a** co-precipitation method and **b** thermal decomposition method

is critical to enhance diagnostic sensitivity. The selected antibody can be incorporated with the MNP surface via direct covalent bonding such as *N*-(3-dimethyllaminopropyl)-*N*′-ethylcarbodiimide hydrochloride/*N*-hydroxysuccinimide (EDC/NHS) chemistry [34], multi-polymer layer reaction as an engineered building block [35], and protein-mediated bonding [36] (Fig. 2) and sufficient coating of the antibody MNP is important to prevent the exposure of the bare MNP surface to the environment, which would lead to MNP alteration and other interactions deteriorating the diagnostic sensitivity.

2.3 Confirmation Method for Bioconjugation of MNPs

To ensure the successful conjugation of antibodies with MNPs, protein estimation is typically followed and most approaches are based on the direct or indirect color change caused by specific binding with a third compound. The Bradford method, which utilizes dye binding to the target protein and subsequent colorimetric monitoring, is the classical protein estimation method [37]. It has been widely adopted in various antibody-conjugated MNPs [38–42] and the antibody-binding efficiency was verified up to 94.5% [7]. A phosphatase method utilizes alkaline phosphatase-linked secondary antibody incubated at room temperature and then conjugated with the primary antibody on the MNP surface. The resultant phosphatase-conjugated antibody–MNPs react with *p*-nitrophenyl phosphate solution and the absorbance can be measured at 405 nm [10]. Other fluorescent linkage methods have been recently introduced for faster and easier protein estimation. For example, a cytometric-based method using herceptin that increases fluorescence intensity was used to confirm antibody conjugation [43].

3 Immunoassays Based on MNPs

In this section, we introduce recent advances in MNP-based immunoassays that can be applied to point-of-care diagnosis. MNPs-based immunoassays are categorized into five types: (1) improvement of the conventional enzyme-linked immunosorbent assay (ELISA), (2) immunoassays based on the peroxidase-like activity of MNPs, (3) MNP–antibody–horseradish peroxidase (HRP) coating method, (4) filtration method, and (5) lateral-flow immunoassay. Figure 3 shows a schematic diagram of each immunoassay. Table 1 summarizes the analytical target, type of MNPs and antibody used for conjugating MNPs, and detection range/detection limit of MNP-based immunoassays. We also provide Table 2 presenting the MNP size used for different types of MNP immunoassays and the achieved detection time.

3.1 MNP-Based ELISA Incorporating Enzyme–Antibody Conjugates

Enzyme-linked immunosorbent assay (ELISA) is a simple, sensitive, and versatile assay mainly for the quantitation of various antigens and antibodies [44]. Conventional ELISA assay has been widely used for decades for analytical methods in viruses [45, 46] and bacteria detection [47, 48], monitoring of environmental pollutants [49, 50], and food allergens [51, 52]. As shown in Fig. 3a, indirect and sandwich types of ELISA are mainly used. In indirect ELISA, antigens are first fixed on the plate well and then the primary antibody and enzyme-conjugated secondary antibody are attached. In the sandwich type of ELISA, captured antibodies are fixed on the plate well, followed by attachment of antigens and primary antibody and enzyme-conjugated secondary antibody are attached in order. While ELISA is simple and cost effective and has high throughput and reproducibility [53], a relatively high detection limit and a long analysis time are the main drawbacks. To improve the shortcomings of ELISA, MNPs have been applied to the immunoassays where they mainly act as solid supports

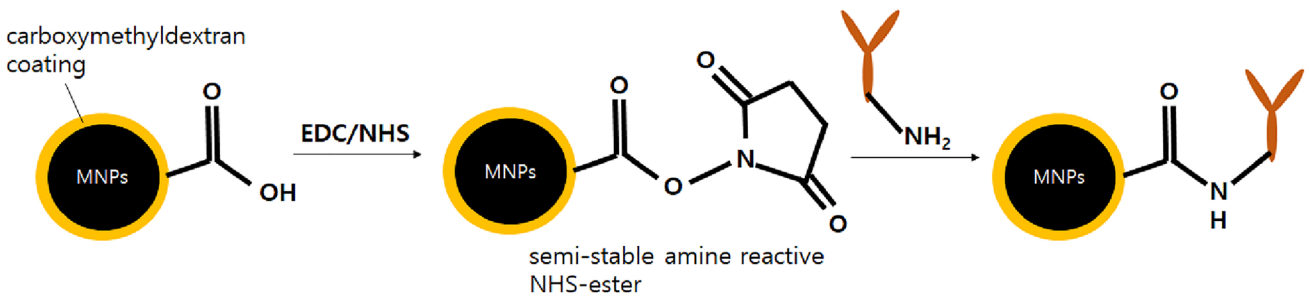

Fig. 2 Schematic illustration of the immobilized native antibody on carboxymethyl-dextran coated MNPs via EDC/NHS chemistry

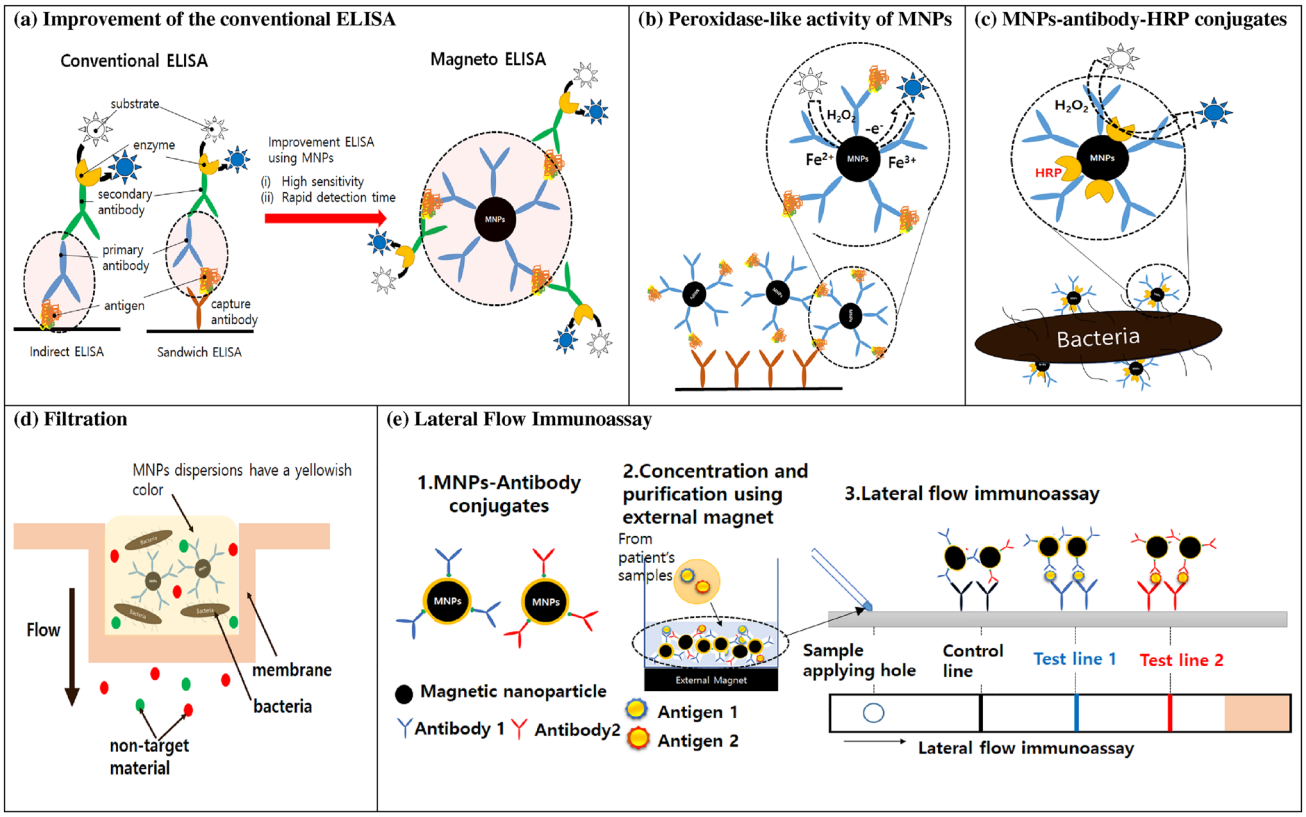

Fig. 3 Schematic illustration of the immunoassays based on the magnetic nanoparticles. **a** Improvement of the conventional ELISA, **b** peroxidase-like activity of MNPs, **c** MNPs–antibody–HRP conjugates, **d** filtration, and **e** lateral-flow immunoassay

for primary antibodies [7–9, 11, 53, 54]. These MNP-based ELISA significantly lowered the detection limits and shortened the analysis time due to the following reasons: (i) the well-dispersed antibody-conjugated MNPs have high surface area, which allows faster reactions between antibodies and antigens, (ii) since MNPs are easily manipulated with an external magnet, antigens captured by antibody-conjugated MNPs can be rapidly separated and preconcentrated, which increases the sensitivity of the immunoassays (Fig. 3a).

For example, Castilho et al., [7] developed magneto-based ELISA for the detection of *Plasmodium falciparum* histidine-rich protein2 (HRP2). They first conjugated IgM monoclonal antibodies onto 300 nm MNPs (anti-HRP2–MNP conjugates). *Plasmodium falciparum* HRP2 proteins were incubated with anti-HRP2–MNP conjugates in 96-well plates, followed by attaching secondary antibodies (anti-HRP2 IgG antibody) labeled with the enzyme horseradish peroxidase (HRP). An external magnet was then applied to collect anti-HRP–MNP conjugates interacting with antigens (*Plasmodium falciparum* HRP2) and secondary antibodies with HRP. A substrate solution that includes H_2O_2 and 3,3′,5,5′-tetramethylbenzidine (TMB), which reacts with HRP to the assay and yields a blue color ($\lambda_{max} = 650$ nm), was then added. Optical measurements were conducted after adding 2 M of H_2SO_4 to stop the enzymatic reaction, which changes the color from blue to yellow ($\lambda_{max} = 450$ nm). The 450 nm absorbance linearly increased with increasing *Plasmodium falciparum* HRP2 concentrations in a range from 0.35 to 7.81 ng mL^{-1} with a limit of detection of 0.35 ng mL^{-1}, which is one order of magnitude lower than other conventional ELISA. Very recently, Sánchez-Cano et al. [8] successfully developed magneto-ELISA for sensitive quantification of *Plasmodium falciparum* lactate dehydrogenase (*Pf*LDH) using ant-PAN *Plasmodium* LDH monoclonal antibody–magnetic bead conjugates, detection antibody, and poly-HRP as an enzymatic signal amplifier and achieved a low detection limit of 0.02 ng mL^{-1} and rapid detection time (< 15 min).

In addition to virus detection, other biomaterials such as bacteria [9], metabolite of mold fungi [53, 54], and food allergens [11] have been analyzed by magneto-ELISA with low detection limits and fast diagnosis times. The MNP size used for developing magneto-ELISA and detection times are summarized in Table 2.

Table 1 Representative MNPs-based immunoassays

Analytical target		Magneto-immunoassay type	MNPs (surface coating/ size)	Antibody conjugated with MNPs	Detection range	Detection limit (LOD in previous studies)	Refs.
Virus	*Plasmodium falciparum* histidine-rich protein 2 (pfHRP2) related to Malaria	Improvement of the conventional ELISA	Polymer-based magnetic nanoparticles (styrene-based copolymer/300 nm)	Anti-*P. falciparum* HRP2 IgM antibody	0.35–7.81 ng mL^{-1}	0.35 ng mL^{-1} (8–80 ng mL^{-1} by immunosensor using different nanoparticles, Sharma et al. [90])	[7]
	Plasmodium falciparum lactate dehydrogenase (PfLDH)	Improvement of the conventional ELISA	Carboxylated modified magnetic beads (-/ 1–3 µm)	Anti-PAN *plasmodium* LDH monoclonal antibody	0.1–25 ng mL^{-1}	0.11 ng mL^{-1}	[8]
	enterovirus 71 (EV71)	Improvement of the conventional ELISA	*N*-hydroxysuccinimide-activated magnetic beads (–/1 µm)	Secondary anti-EV71 antibody conjugated with acetylcholinesterase (AChE)	10^4–10^8 copies mL^{-1}	Lowest concentration where the color change can be discriminated by the naked eye: 10^4 copies mL^{-1} (10^4 copies mL^{-1} by real-time PCR; 10^8 copies mL^{-1} by conventional ELISA)	[91]
	Enterovirus 71 (EV71) Coxsackievirus B3 (CVB3)	Improvement of the conventional ELISA	Superparamagnetic carboxyl-Adembeads (–/ 411–439 nm)	EV71 monoclonal antibody CVB3 monoclonal antibody	EV71: 3.0×10^3–4.0×10^4 copies mL^{-1} CVB3: 2.0×10^3–3.0×10^4 copies mL^{-1}	EV71: 1716 copies mL^{-1} CVB3: 1618 copies mL^{-1}	[92]
	Potato virus X	Lateral-flow immunoassay	Carboxylate MNPs	Monoclonal antibody (clone 3G4) specific for potato virus X	0.25–125 ng mL^{-1}	0.25 ng mL^{-1}	[78]
Bacteria	*Escherichia coli* (*E. coli*)	Improvement of the conventional ELISA	Silanized magnetic nanoparticles (SiO_2/60–300 nm)	Monoclonal antibody IgG 2a 898 anti-common enterobacterial antigen (ECA)	–	2.6×10^5 cells mL^{-1} (10^6 cells mL^{-1} from ELISA based on ECA antibody, [93])	[9]
	Salmonella typhimurium	MNPs–antibody–HRP coating method	Silica shell magnetic nanoparticles (treatment with (3-aminopropyl)triethoxysilane (APTES)-produced surface amino-group/ 90 nm)	Goat polyclonal anti-*S. typhimurium* antibody	0–10^4 colony forming units (CFU)	10 colony forming unit (CFU)	[10]
	Escherichia coli O157:H7	Filtration	Magnetic nanoparticles (caboxymethyldextran/ 100 nm)	Biotinylated anti-*E. coli* O157:H7 antibody	5–10^4 colony forming units (CFU) mL^{-1}	10 colony forming units (CFU) mL^{-1} through visual observation	[65]
	Staphylococcus aureus (*S. aureus*)	Filtration	Magnetic nanoparticles (caboxymethyl-dextran/ 100 nm) *. Gold nanoparticle (AuNP) conjugated with MNPs	Anti-*S. aureus* antibody *. Antibody directly conjugated with AuNPs		1.5×10^3 colony forming units (CFU) in phosphate buffer saline (PBS) 1.5×10^5 colony forming units (CFU) in the milk sample	[66]

Table 1 (continued)

Analytical target		Magneto-immunoassay type	MNPs (surface coating/size)	Antibody conjugated with MNPs	Detection range	Detection limit (LOD in previous studies)	Refs.
Food allergen	Ara h3/4 peanut allergen	Improvement of the conventional ELISA	Magnetic particles activated with a primary amine (PAMAM dendrimers, 2.8 μm)	Anti-Ara h3/4 (Pn-b) monoclonal immunoglobulins G antibody	2.5–15 mg peanuts kg^{-1} matrix	0.2 mg peanuts kg^{-1} matrix	[11]
	Ara h1 peanut allergen	Lateral-flow immunoassay	Carboxylic acid magnetic nanoparticles (–/100–200 nm)	Anti-Ara h1 antibody	0.01–2.5 μg mL^{-1} (Ara 1 in PBS)	0.01 μg mL^{-1} (Ara 1 in PBS) 5.625 mg kg^{-1} peanut protein Commercial ELISA kits: 10 mg kg^{-1} peanut protein [94]	[67]
Others	Prostate-specific antigen (PSA)	Using peroxidase-like activity of MNPs	Carboxyl-functionalized iron oxide nanoparticles (-, 30 nm)	Polyclonal rabbit antihuman PSA antibody	1.0–64.0 ng mL^{-1}	1.0 ng mL^{-1} Clinical diagnostic threshold: 4.0 ng mL^{-1} [95, 96]	[58]
	Human chorionic gonadotropin (hCG)	Using peroxidase-like activity of MNPs	NH_2-functionalized magnetic nanoparticles (–, 15 nm)	Anti-human chorionic gonadotropin (hCG) β antibody	Only test with 50 ng mL^{-1} hCG antigen	N.A.[a]	[56]
	Carcinoembryonic antigen (CEA)	Lateral-flow immunoassay	Carboxyl-functionalized MNPs (–, 200 nm)	Anti-CEA monoclonal antibody	0.25–1000 ng mL^{-1}	0.25 ng mL^{-1} from human serum sample Commercial electrochemiluminescence immunoassay (ECLIA): 5 ng mL^{-1} from human serum sample	[76]
	Aflatoxin B1 (AFB1)	Improvement of the conventional ELISA	Magnetic nanoparticles (–/10 nm)	Anti-AFB1 antibody	0.002–0.2 ng mL^{-1}	0.002 ng mL^{-1} (conventional ELISA: 0.015 ng mL^{-1})	[53]

Table 2 MNP size used for magneto-immunoassay and achieved detection time from previous studies

Magneto-immunoassay type	MNPs size (nm) *. Blue bar shows the MNP size ranges of each type and red mark represents the MNP size used in each reference	Detection time	Refs.
Modification of conventional ELISA		15–45 min	[7, 8, 53, 91, 92]
Immunoassays based on the peroxidase-like activity of MNPs	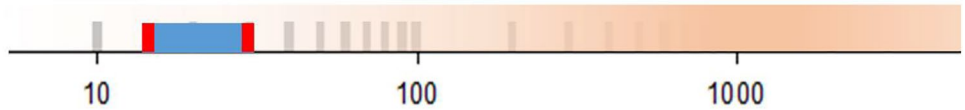	N.A.[a]	[56, 58]
MNPs–antibody–HRP coating method		N.A.[a]	[10, 63]
Filtration		40–55 min	[65, 66]
Lateral-flow immunoassay	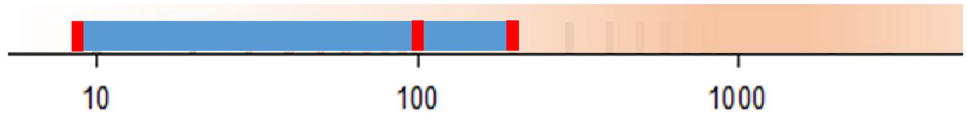	15 min	[67, 79]

[a]Not available

3.2 Immunoassays Based on the Peroxidase-Like Activity of MNPs

As described in Sect. 3.1, both conventional ELISA and magneto-ELISA use enzymes such as horseradish peroxidase (HRP) for the color development resulting from the catalytic activity. However, in 2007, Yan's group first discovered that MNPs themselves have intrinsic peroxidase-like activity, as Fe^{2+} /Fe^{3+} ions on the surfaces of MNPs can act as a catalyst for the breakdown of hydrogen peroxidase [55]. Indeed, they showed that MNPs oxidize various peroxidase substrates such as 3,3′,5,5′-tetramethylbenzidine (TMB), diazo-aminobenzene (DAB), and *o*-phenylenediamine (OPD) in the presence of H_2O_2, and the optimal catalytic activity appeared at pH 3.5 and 40 °C, which are very similar to the optimal conditions for HRP. Thus, for immunoassay application, MNPs are not only magnetic separators, but also excellent representatives for HRP, and they are more stable than HRP over a broad range of temperature and pH [55]. A schematic illustration for the peroxidase-like activity of MNPs is shown in Fig. 3b.

After this discovery, many efforts have been made to develop immunoassays using the peroxidase-like activity of MNPs. For example, Yang et al. [56] showed that amino-functionalized MNPs possess high peroxidase-like activity, and the optimal pH and temperature for the activity are pH 4 and 40 °C. They successfully conducted colorimetric detection of human chorionic gonadotropin (hCG) using anti-hCG β-conjugated amino-functionalized MNPs (size: 15 nm) without HRP usage. MNPs with reactive amino groups on their surfaces (size: 10 nm) were applied to a colorimetric immunoassay for detecting rotavirus with a significant reduction of the limit of detection (LOD) of rotavirus compared to the conventional ELISA method. Woo et al. [57] detected human breast cells with a slightly higher LOD than the ELISA method; however, the MNP-based immunoassays take less time than ELISA method because the direct immunoassay does not require any cell lysis procedure. Fu et al. [58] used 30 nm carboxyl-functionalized MNPs for colorimetric detection of prostate-specific antigen (PSA) based on TMB–H_2O_2 color development generated by the peroxidase activity of MNPs. The color development (UV–Vis absorbance at 650 nm) linearly increased with increasing PSA concentrations (0–64.0 ng mL^{-1}). This is because the higher the PSA concentration, the greater is the number of MNPs captured by the capture antibody. On the other hand, without using captured antibody, the color development can decrease with increasing target concentration. For example, when 30 nm chitosan-coated MNPs were incubated with the *Escherichia coli* and *Staphylococcus aureus*, the color development significantly reduced because the peroxidase-like activity was hindered by the interaction of the bacteria with positively charge MNPs [59]. It is noteworthy that the size of MNPs based on their peroxidase-like activity ranged from 10 to 30 nm, which is small compared with MNPs applied to the modified ELISA method (Table 2); this is possibly due to (i) smaller MNPs having higher peroxidase-like activity due to the high surface to volume ratio, and (ii) it being easy to remove unbound smaller MNPs during the washing step.

Recently, the enzymatic activity of MNPs has been broadly utilized in a wide range of applications such as detection of various biomolecules including glucose, galactose, ascorbic acid [60], nucleic acids [61], and chemicals such as alcohols [62].

3.3 MNPs–Antibody–HRP Coating Method

Since the application of MNPs to the classical ELISA sandwich assay requires at least two antibodies (e.g., an antibody conjugated with MNPs and a secondary antibody conjugated with enzymes or fluorescent dyes) and various serial steps, it takes a relatively long time (i.e., more than several hours) and the method is complicated for point-of-care detection. To simplify the detection method, Baldrich et al. proposed dually labeled magnetic particles that are simultaneously conjugated with both the antibody and enzyme [63] (Fig. 3c). To detect *Escherichia coli* (*E. coli*), they synthesized dually labeled magnetic particles (diameter: 1 μm) by coating anti-*E. coli* antibody and HRP in a molar ratio of 1:3. With a large target such as bacteria, the target conjugation with dually coated magnetic particles generated "enzyme shadowing effects", which means interactions between nanoparticles and bacteria reduces enzymatic activity by blocking enzyme substrate access. Color development through enzyme reactions thus decreased with increasing bacteria concentrations, and the signal decrease was proportional to the bacterial concentration within a range of 10^3–10^4 cell mL^{-1} within 1 h [63], which resulted in a fast one-step immunoassay. The advantage of applying the dually labeled magnetic particles to the immunoassay is that it achieves rapid detection by capturing and reporting the target materials at the same time. In addition, by minimizing the detection process, it is possible to obtain reproducible results by preventing the loss of magnetic nanoparticles in the washing steps, which are essential in the MNP-based ELISA.

Mun and Choi [10] also applied dually labeled MNPs (diameter: 100 nm) to detect *Salmonella typhimurium,* but they enhanced the detection sensitivity by using filtration and modifying detection systems. The MNPs were first conjugated with anti-*S. typhimurim* antibody and HRP with a molar ratio of 1:10 (MNP–Ab–HRP). MNP–Ab–HRP was then incubated with *Salmonella typhimurium,* followed by passing through a 0.6 μm polycarbonate track-etched (PCTE) filter to separate bacteria-bound MNP–Ab–HRP from unbound MNPs. The HRP activity from remaining bacteria-bound MNP–Ab–HRP was measured by a luminometer

system. Since the light intensity of the system is generated by particle binding to bacteria via antibody mediation, the resultant light intensity increased with increasing bacteria concentration with a lower detection limit (10 CFU) and fast process time (less than 10 min).

In addition to bacteria detection, dually labeled magnetic nanoparticles have recently been applied for virus detection [1, 62]. Li and Lillehoj [64] developed an alternating current electrothermal flow (ACEF)-enhanced magneto-immunosensor to detect *Plasmodium falciparum* histidine-rich protein 2 (*Pf* HRP2). They synthesized dually labeled MNPs (carboxylated magnetic nanobeads, diameter: 200 nm) which were conjugated with HRP and HRP-conjugated anti-*Pf* HRP2 IgG antibodies at 200:1 molar ratio. ACEF mixing was applied to the sensor to enhance antigen transport and formation of antigen–MNPs immunocomplexes, followed by adding TMB substrate to generate an amperometric current. It was reported that additional coating of HRP on the dually labeled MNPs effectively increased the amperometric signal, decreasing the detection limit. The sensor achieved ultrafast detection time (~ 7 min) as well as low detection limit (5.7 pg mL^{-1} *Pf* HRP2 in whole blood). The dually labeled magnetic nanoparticles were also used to detect SARS-CoV-2N protein incorporating with microfluidic chips [1], and the details are described in Sect. 4.

3.4 Filtration

Since antibody-conjugated MNPs selectively attach to the target analytes and the size of target–MNPs complexes is larger than the unbound materials (e.g., unbound target, unbound MNPs, and non-target materials), filtration easily separates the target–MNPs complexes and unbound materials. In addition, since the MNPs dispersions are yellowish, as more target MNPs remain on the filter support, they show more color development and are easily identified with the naked eye. The immunoassay using filtration is schematically shown in Fig. 3d.

Kim et al. [65] used filtration for naked eye detection of *E. coli* O157:H7. They synthesized biotinylated anti-*E. coli* O157:H7 antibody/streptavidin–alkaline phosphatase (STA–AP)/MNP conjugates, and then captured and purified *E. coli* O157:H7 with biotinylated anti-*E. coli*/STA-SP/MNP conjugates. A 1.2 µm nitrocellulose membrane filter equipped with a fitted glass support under vacuum pressure effectively separated the target–bacteria conjugates (which is larger than 1.2 µm) from unbound anti-*E. coli*/STA–SP/MNP conjugates. Normal color intensity of bacteria–MNP conjugates remaining on the filter increased with increasing bacteria concentration from 10 to 10^4 CFU mL^{-1}, and the color can enzymatically amplify with nitroblue tetrazolium (NBT)/5-bromo-4-chloro-3-indolyl phosphate (BCIP) precipitation. The filtration method was also used in Sung et al. [66] study for rapid colorimetric detection of *Staphylococcus aureus* (*S. aureus*) in PBS buffer as well as milk. To separate *S. aureus*-bound MNPs complex from unbound MNPs, 0.8 µm cellulose acetate membrane filters were used. In this study, gold nanoparticles also conjugated with MNPs for color amplification, and they reported that the resultant assay showed high sensitivity with a detection limit of 1.5×10^3 for *S. aureus* in PBS buffer as well as fast detection time of only 40 min.

3.5 Lateral-Flow Immunoassay

The lateral-flow immunoassay (LFIA) is a rapid, cost-effective, and convenient diagnostic method and widely used for point-of-care detection [67]. Conventional LFIA pads consist of a sample pad, a conjugate pad containing capture antibodies specified for target antigens, a nitrocellulose membrane with two capture antibodies for targets (test line) and detection antibodies (control line), and an absorbent pad. Recently, various types of nanoparticles such as gold [68–71], quantum dots [72, 73] and silica nanoparticles [74, 75] have been applied to the LFIA to increase its sensitivity and stability. Among various nanoparticles, MNPs are also considered attractive materials for the development of accurate and sensitive LFIA for the point-of-care detection for the following reasons: (1) Due to the superparamagnetic property of MNPs, target materials can be rapidly concentrated and separated from impurities prior to application to LFIA. This significantly increases the detection sensitivity and reduces matrix interferences and detection time [5, 76]. (2) MNP dispersions exhibit a strong brownish yellow color and the color intensity increases with the formation of MNP aggregates. Therefore, MNP–target material complexes serve as color signals in the MNPs incorporating LFIA, simplifying the detection process. (3) Because MNPs have stable physical properties over a wide range of temperature, pH, and ionic strength, MNPs incorporating LFIA can be applicable to regions with harsh environmental condition compared to the conventional LFIAs. (4) Signal visibility of MNPs incorporating LFIA can be easily enhanced by conjugating MNPs with other materials such as gold nanoparticles and quantum dots. (5) quantitative detection of MNPs incorporating LFIA is possible through reading magnetic signals which are stable and highly reproducible [77].

Different from conventional LFIA assays, many MNP-based LFIA follows two steps: (i) target materials are mixed with MNPs conjugated with antibody-forming immune complexes followed by applying an external magnet to enrich and purify the immune complexes, and (ii) the immune complexes are directly applied to the test strip of LFIA, which only consists of a working membrane and an absorbent pad (sample and conjugate pads are not needed, since the immune complexes already contain samples and

MNPs with the capture antibody) (Fig. 3e). For example, Yin et al. [12] developed MNP-based LFIA for detecting the peanut allergen Ara h1. They first synthesized anti-Ara h1 antibody-conjugated MNPs and then mixed then with samples containing Ara h1 to form MNP–Ara h1 immunocomplexes. In this step, an external magnet was applied to isolate and concentrate the MNP–Ara h1 complexes. The samples were resuspended in a running buffer and directly applied to the LFIA test strip. The brown-yellow color successfully appeared both in test and control lines due to the interaction between antibodies immobilized in the test strip and the MNP–Ara h1 complexes, and the color intensity linearly increased with increasing Ara h1 concentration in the range of 0.01–2.5 μg mL^{-1}. They also reported an improved limit of detection of Ara h1 in PBS (0.01 μg mL^{-1}) as well as Ara h1 from various food samples such as cookies, milk, and chocolate. This same type of modified LFIAs based on MNPs also effectively detected various target materials such as major fish allergen parvalbumin [77], potato virus X [78], and mycotoxins [79] with lower visual detection limits compared with conventional LFIAs or ELISA.

4 Recent Advances of Applications of MNPs Immunoassays for COVID-19 Diagnosis

The ongoing coronavirus (COVID-19) pandemic is an urgent threat to global health care, with 446,671,399 confirmed cases including 6,024,328 deaths globally, as of March 7, 2022 [80]. Since the symptoms of COVID-19 are various, ranging from mild flu symptoms to life-threatening diseases, it is critical to detect COVID-19 at an early stage without a false-negative or -positive result [81]. In addition, detecting antibodies against COVID-19 is also imperative for identifying people who already have immunity and avoid them being quarantined [82]. Currently, reverse transcription polymerase chain reaction (RT-PCR) is a standard method for detecting severe acute respiratory syndrome coronavirus 2 (SARS-CoV-2). Although the RT-PCR method is highly sensitive for detecting SARS-CoV-2, it requires expensive laboratory instrumentations, trained technicians, and tedious labor [1, 81]. Thus, for COVID-19 point-of-care application, not only high sensitivity but also rapid time and less labor for detection are required. Currently, many efforts [83–88] have been made to detect SARS-CoV-2 proteins (e.g., SARS-CoV-2 nucleocapsid (N) protein and SARS-CoV-2 spike (S) protein) as well as SARS-CoV-2 antibodies (e.g., SARS-CoV-2 immunoglobulin G and M), but higher sensitivity and faster detection time are still required. In this sense, the application of MNPs to COVID-19 detection is attractive due to

Table 3 Recent development of MNPs immunoassays for the detection of SARS-CoV-2

Target biomarker	MNPs (coating materials/size)	Biomolecules conjugated with MNPs	Magneto-immunoassay type Detection method	Strength	Refs.
Severe acute respiratory syndrome coronavirus 2 (SARS-CoV-2) nucleocapsid protein	Carboxylated magnetic nanobead (–/200 nm)	Detection antibody and HRP (400:1 molar ratio)	MNPs–antibody–HRP coating method Electrochemical measurement with potentiostat	(1) Rapid detection time (< 1 h) and high sensitivity (LOD of 50 pg mL^{-1} from whole serum) (2) Effective antigen enrichment using an external magnet (3) Point-of-care detection utilizing a portable smartphone	[1]
Human IgG antibody present in blood or serum from COVID-19 patient	MagneHis Ni^{2+} magnetic beads (obtained from Premega, particle size is not described by the manufacturer)	Recombinant 6xHis-tagged SARS-CoV-2 Nucleocapsid protein	Improvement of the conventional ELISA Optical density measurement (650 nm)	(1) Cost-effective (cost less than $3) and rapid detection time (< 12 min) (2) Better intraassay reproducibility (CV 2–3%) than the conventional ELISA method (3) High specificity (> 98%) and sensitivity (> 83%)	[89]

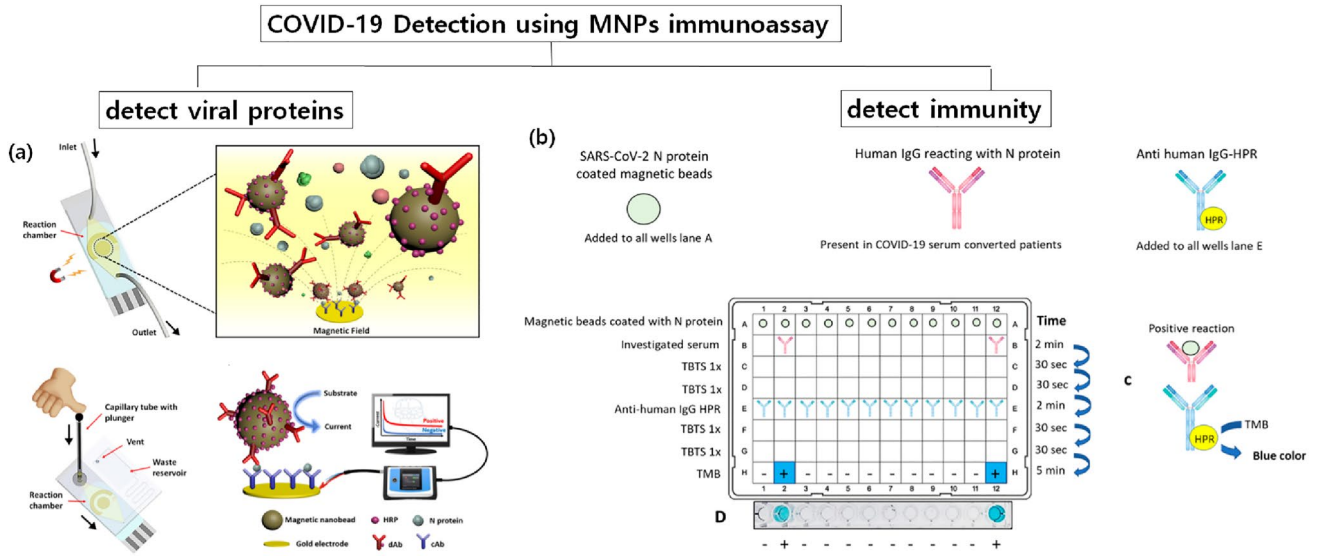

Fig. 4 Schematic illustration of recent advances in MNP-based immunoassays for COVID-19. **a** Method for detecting viral proteins and **b** method for detecting immunity. Figure 2a reprinted with permission from Li and Lillehoj [1] Copyright © American Chemical Society and Figure 2b reprinted with permission from Huergo et al. [89] Copyright © American Chemical Society

mainly two reasons: (i) MNPs have high surface areas that increase sensitivity and several steps including purification, antibody–antigen interactions, and washing steps can be easily combined into one step using an external magnet. As far as we are aware, there are two magneto-immunosensors applied for COVID-19 diagnosis and Table 3 summarizes the size and coating materials of MNPs, magneto-immunoassay type, and strength of the diagnosis methods.

Li and Lillehoj [1] developed a magneto-immunosensor for detecting SARS-CoV-2N protein in whole serum using MNP–antibody–HRP conjugates (in the paper, they refer to it as dually labeled magnetic nanobeads (DMBs)). They used carboxylated magnetic MNPs (200 nm) and detection antibody and HRP at a molar ratio of 400:1 conjugated with MNPs. The thiolated captured antibody was immobilized on screen-printed gold electrode (SPGE) sensors and then inserted into a microfluidic chip. The use of microfluidic chips incorporating MNPs and an external magnet significantly increased the interaction between the antibody and antigen while enhancing the detection sensitivity. In addition, combining all detection processing in the chip reduces labor and detection time. As shown in Fig. 4a, in the microfluidic chip, the sample containing SARS-CoV-2N proteins was mixed with DMBs to form SARS-CoV-2N–DMBs complexes. The complexes moved to the sensor and then rapidly bound to the captured antibodies with the help of the external magnet. With a TMB substrate solution, HRP, which was conjugated with DMBs, reacts with the TMB. This created color as well as amperometric current, which linearly increased with increasing antigen concentrations. Using this MNPs immunoassay, SARS-CoV-2N proteins were detected at levels as low as 50 pg mL^{-1} in undiluted whole serum within 55 min. The sensors were connected with a smartphone-based sensing device, allowing quantitative and user-friendly point-of-care detection.

In addition to detecting viral proteins, which indicates current virus infection, detecting antibodies against SARS-CoV-2 is important to distinguish people who already have been infected. Antibody detection is especially critical for COVID-19, since the viral infection of SARS-CoV-2 shows very minor and negligible symptoms for many cases and people do not know whether they have healthy immune systems against COVID-19. Once it is confirmed that people have been infected with COVID-19 via antibody-detecting tests, they can return to work without any risks [82]. From this point of view, Huergo et al. [89] developed an MNP-based immunoassay for detecting human SARS-CoV-2 antibodies. They first purified SARS-CoV-2N protein and coated magnetic beads with proteins. The antigen-coated magnetic beads were then distributed into the wells of a 96-well plate and mixed with 2 µL of diluted human serum or 5 µL of diluted human blood for 2 min. After several washing steps, the MNP beads were incubated with goat-anti-human IgG-HPR captured antibody, followed by incubation with TMB substrate for color development. The MNP beads were captured and released at each step using a magnetic extractor device (Fig. 4b). They confirmed that only positive COVID-19 samples develop a color, suggesting human IgG antibody from COVID-9 patients effectively combined with SARS-CoV-2N protein. This immunoassay showed almost the same detection range as the standard ELISA method, and high sensitivity (more than 83%) as well as high specificity

(more than 98%) was obtained by analyzing samples from two independent laboratories. Since selecting appropriate antigens is the most important and difficult task for detecting antibodies [82], further studies are necessary for finding and purifying antigens considering virus mutation.

5 Conclusions and Future Perspectives

Currently, immunoassay-based rapid detection kits have been remarkably developed for detecting various target analytes. However, improvements in sensitivity and specificity are still desired to prevent disease transmission as well as to lower detection limits from very low target concentrations. MNPs are attractive materials to achieve high sensitivity of detection due to their unique properties such as magnetic behaviors, biocompatible characteristics, and high surface areas. In addition, MNPs are very suitable materials for detection of diseases by color development, since MNPs themselves possess representative enzymatic peroxidase activity or they can stably conjugate materials for color expression. Different types of MNP-based immunoassays are applicable to user-friendly POC detection via color development. Recent efforts for COVID-19 diagnosis via MNP-based immunoassays have led to their improvements over conventional diagnosis methods. Considering that MNPs are easily produced with low cost, while having high thermal and pH stability compared to other enzymatic materials commonly used for detection kits, assays incorporating MNPs are also expected to be applicable in developing countries and remote regions where temperature and humidity are harsh factors impeding detection.

Acknowledgements This research was supported by the Basic Science Research Program through the National Research Foundation of Korea (NRF-2020R1I1A1A01069283).

Declarations

Conflict of Interest The authors declare no competing financial interest.

References

1. Li, J., Lillehoj, P.B.: Microfluidic magneto immunosensor for rapid, high sensitivity measurements of SARS-CoV-2 Nucleocapsid protein in serum. ACS Sens. **6**, 1270–1278 (2021)
2. Ramdas, K., Darzi, A., Jain, S.: 'Test, re-test, re-test': using inaccurate tests to greatly increase the accuracy of COVID-19 testing. Nat. Med. **26**, 810–811 (2020)
3. Kevadiya, B.D., Machhi, J., Herskovitz, J., Oleynikov, M.D., Blomberg, W.R., Bajwa, N., Soni, D., Das, S., Hasan, M., Patel, M.: Diagnostics for SARS-CoV-2 infections. Nat. Mater. **20**, 593–605 (2021)
4. Xu, C., Akakuru, O.U., Zheng, J., Wu, A.: Applications of iron oxide-based magnetic nanoparticles in the diagnosis and treatment of bacterial infections. Front. Bioeng. Biotechnol. **7**, 141 (2019)
5. Ha, Y., Ko, S., Kim, I., Huang, Y., Mohanty, K., Huh, C., Maynard, J.A.: Recent advances incorporating superparamagnetic nanoparticles into immunoassays. ACS Appl. Nano Mater. **1**, 512–521 (2018)
6. Gowri, A., Kumar, A., Anand, B.S.S.: Recent advances in nanomaterials based biosensors for point of care (PoC) diagnosis of covid-19—a minireview. TrAC Trends Anal. Chem. **137**, 116205 (2021)
7. de Souza Castilho, M., Laube, T., Yamanaka, H., Alegret, S., Pividori, M.: Magneto immunoassays for *Plasmodium falciparum* histidine-rich protein 2 related to malaria based on magnetic nanoparticles. Anal. Chem. **83**, 5570–5577 (2011)
8. Sánchez-Cano, A., Ruiz-Vega, G., Vicente-Gómez, S., de la Serna, E., Sulleiro, E., Molina, I., Sánchez-Montalvá, A., Baldrich, E., Baldrich, E.: Development of a fast chemiluminescent magneto-immunoassay for sensitive *Plasmodium falciparum* detection in whole blood. Anal. Chem. **93**, 12793–12800 (2021)
9. Pappert, G., Rieger, M., Niessner, R., Seidel, M.: Immunomagnetic nanoparticle-based sandwich chemiluminescence-ELISA for the enrichment and quantification of *E. coli*. Microchim. Acta **168**, 1–8 (2010)
10. Mun, S., Choi, S.-J.: Detection of *Salmonella typhimurium* by antibody/enzyme-conjugated magnetic nanoparticles. BioChip J. **9**, 10–15 (2015)
11. Speroni, F., Elviri, L., Careri, M., Mangia, A.: Magnetic particles functionalized with PAMAM-dendrimers and antibodies: a new system for an ELISA method able to detect Ara h3/4 peanut allergen in foods. Anal. Bioanal. Chem. **397**, 3035–3042 (2010)
12. Yin, H.-Y., Li, Y.-T., Tsai, W.-C., Dai, H.-Y., Wen, H.-W.: An immunochromatographic assay utilizing magnetic nanoparticles to detect major peanut allergen Ara h 1 in processed foods. Food Chem. **375**, 131844 (2022)
13. Kim, H., Lee, S., Seo, H.W., Kang, B., Moon, J., Lee, K.G., Yong, D., Kang, H., Jung, J., Lim, E.-K., Jeong, J., Part, H.G., Ryu, C.-M., Kang, T.: Clustered regularly interspaced short palindromic repeats-mediated surface-enhanced Raman scattering assay for multidrug-resistant bacteria. ACS Nano. **14**, 17241–17253 (2020)
14. Cai, Q., Wang, R., Qiao, Z., Yang, W.: Single-digit Salmonella detection with the naked eye using bio-barcode immunoassay coupled with recombinase polymerase amplification and a CRISPR-Cas12a system. Analyst **146**, 5271 (2021)
15. Pastucha, M., Farka, Z., Lacina, K., Mikušová, Z., Skládal, P.: Magnetic nanoparticles for smart electrochemical immunoassays: a review on recent developments. Microchim. Acta **186**, 1–26 (2019)
16. Kavetskyy, T., Alipour, M., Smutok, O., Mushynska, O., Kiv, A., Fink, D., Farshchi, F., Ahmadian, E., Hasanzadeh, M.: Magneto-immunoassay of cancer biomarkers: recent progress and challenges in biomedical analysis. Microchem. J. **167**, 106320 (2021)
17. Cao, B., Wang, K., Xu, H., Qin, Q., Yang, J., Zheng, W., Jin, Q., Cui, D.: Development of magnetic sensor technologies for point-of-care testing: fundamentals, methodologies and applications. Sens. Actuators A **312**, 112130 (2020)
18. Hyeon, T.: Chemical synthesis of magnetic nanoparticles. Chem. Commun. **2003**, 927–934 (2003)
19. Frey, N.A., Peng, S., Cheng, K., Sun, S.: Magnetic nanoparticles: synthesis, functionalization, and applications in bioimaging and magnetic energy storage. Chem. Soc. Rev. **38**, 2532–2542 (2009)
20. Moradnia, F., Fardood, S.T., Ramazani, A., Min, B.-K., Joo, S.W., Varma, R.S.: Magnetic $Mg_{0.5}Zn_{0.5}FeMnO_4$ nanoparticles: green

sol-gel synthesis, characterization, and photocatalytic applications. J. Clean. Prod. **288**, 125632 (2021)
21. Marcelo, L.R., de Gois, J.S., da Silva, A.A., Cesar, D.V.: Synthesis of iron-based magnetic nanocomposites and applications in adsorption processes for water treatment: a review. Environ. Chem. Lett. **19**, 1229–1274 (2021)
22. Massart, R.: Preparation of aqueous magnetic liquids in alkaline and acidic media. IEEE Trans. Magn. **17**, 1247–1248 (1981)
23. Mornet, S., Vasseur, S., Grasset, F., Veverka, P., Goglio, G., Demourgues, A., Portier, J., Pollert, E., Duguet, E.: Magnetic nanoparticle design for medical applications. Prog. Solid State Chem. **34**, 237–247 (2006)
24. Li, L., Fan, M., Brown, R.C., Van Leeuwen, J., Wang, J., Wang, W., Song, Y., Zhang, P.: Synthesis, properties, and environmental applications of nanoscale iron-based materials: a review. Crit. Rev. Environ. Sci. Technol. **36**, 405–431 (2006)
25. Kim, I., Best, C., Kim, S.: Feasibility of electromagnetic soil heating using magnetic nanoparticle-coated geotextiles. Geotech. Lett. **10**, 149–154 (2020)
26. Sun, Y., Li, X., Zheng, W.: Facile synthesis of core-shell phase-transited lysozyme coated magnetic nanoparticle as a novel adsorbent for Hg (II) removal in aqueous solutions. J. Hazard. Mater. **403**, 124012 (2021)
27. Hyeon, T., Lee, S.S., Park, J., Chung, Y., Na, H.B.: Synthesis of highly crystalline and monodisperse maghemite nanocrystallites without a size-selection process. J. Am. Chem. Soc. **123**, 12798–12801 (2001)
28. Papaefthymiou, G.C.: Nano Today **4**, 438–447 (2009)
29. Zhu, Y., Kekalo, K., Dong, C., Huang, Y.Y., Shubitidze, F., Griswold, K.E., Baker, I., Zhang, J.X.: Magnetic-nanoparticle-based immunoassays-on-chip: materials synthesis, surface functionalization, and cancer cell screening. Adv. Funct. Mater. **26**, 3953–3972 (2016)
30. Plouffe, B.D., Murthy, S.K., Lewis, L.H.: Fundamentals and application of magnetic particles in cell isolation and enrichment: a review. Rep. Prog. Phys. **78**, 016601 (2014)
31. Laurent, S., Dutz, S., Häfeli, U.O., Mahmoudi, M.: Magnetic fluid hyperthermia: focus on superparamagnetic iron oxide nanoparticles. Adv. Colloid Interface Sci. **166**, 8–23 (2011)
32. Kievit, F.M., Zhang, M.: Surface engineering of iron oxide nanoparticles for targeted cancer therapy. Acc. Chem. Res. **44**, 853–862 (2011)
33. Ndong, C., Toraya-Brown, S., Kekalo, K., Baker, I., Gerngross, T.U., Fiering, S.N., Griswold, K.E.: Antibody-mediated targeting of iron oxide nanoparticles to the folate receptor alpha increases tumor cell association in vitro and in vivo. Int. J. Nanomed. **10**, 2595 (2015)
34. Richard, S., Boucher, M., Herbet, A., Lalatonne, Y., Mériaux, S., Boquet, D., Motte, L.: Endothelin B receptors targeted by iron oxide nanoparticles functionalized with a specific antibody: toward immunoimaging of brain tumors. J. Mater. Chem. B. **3**, 2939–2942 (2015)
35. Fiandra, L., Mazzucchelli, S., De Palma, C., Colombo, M., Allevi, R., Sommaruga, S., Clementi, E., Bellini, M., Prosperi, D., Corsi, F.: Assessing the in vivo targeting efficiency of multifunctional nanoconstructs bearing antibody-derived ligands. ACS Nano **7**, 6092–6102 (2013)
36. Gallo, J., García, I., Genicio, N., Padro, D., Penadés, S.: Specific labelling of cell populations in blood with targeted immunofluorescent/magnetic glyconanoparticles. Biomaterials **32**, 9818–9825 (2011)
37. Bradford, M.M.: A rapid and sensitive method for the quantitation of microgram quantities of protein utilizing the principle of protein-dye binding. Anal. Biochem. **72**, 248–254 (1976)
38. Abdolahi, M., Shahbazi-Gahrouei, D., Laurent, S., Sermeus, C., Firozian, F., Allen, B.J., Boutry, S., Muller, R.N.: Synthesis and in vitro evaluation of MR molecular imaging probes using J591 mAb-conjugated SPIONs for specific detection of prostate cancer. Contrast Media Mol. Imaging **8**, 175–184 (2013)
39. Jo, S.-M., Noh, S.-H., Jin, Z., Lim, Y., Cheon, J., Kim, H.-S.: Simple and efficient capture of EGFR-expressing tumor cells using magnetic nanoparticles. Sens. Actuators B Chem. **201**, 144–152 (2014)
40. Truffi, M., Colombo, M., Sorrentino, L., Pandolfi, L., Mazzucchelli, S., Pappalardo, F., Pacini, C., Allevi, R., Bonizzi, A., Corsi, F.: Multivalent exposure of trastuzumab on iron oxide nanoparticles improves antitumor potential and reduces resistance in HER2-positive breast cancer cells. Sci. Rep. **8**, 1–11 (2018)
41. Krasteva, D.R., Ivanov, Y.L., Chervenkov, T.G., Gabrovska, K.I., Godjevargova, T.I.: $CD34^{+}$ stem cell counting using labeled immobilized anti-CD34 antibody onto magnetic nanoparticles and EasyCounter BC image cytometer. Anal. Biochem. **610**, 113929 (2020)
42. Gunasekaran, D., Gerchman, Y., Vernick, S.: Electrochemical detection of waterborne bacteria using bi-functional magnetic nanoparticle conjugates. Biosensors **12**, 36 (2022)
43. Haghighi, A.H., Faghih, Z., Khorasani, M.T., Farjadian, F.: Antibody conjugated onto surface modified magnetic nanoparticles for separation of HER2+ breast cancer cells. J. Magn. Magn. Mater. **490**, 165479 (2019)
44. Reen, D.J.: Enzyme-Linked Immunosorbent Assay (ELISA). Basic Protein and Peptide Protocols, pp. 461–466. Humana Press, Totowa (1994)
45. Voller, A., Bartlett, A., Bidwell, D., Clark, M., Adams, A.: The detection of viruses by enzyme-linked immunosorbent assay (ELISA). J. Gen. Virol. **33**, 165–167 (1976)
46. Dichtl, K., Zimmermann, J., Koeppel, M.B., Böhm, S., Osterman, A.: Evaluation of a novel CLIA monotest assay for the detection of anti-hepatitis E virus-IgG and IgM: a retrospective comparison with a line blot and an ELISA. Pathogens **10**, 689 (2021)
47. Pang, B., Zhao, C., Li, L., Song, X., Xu, K., Wang, J., Liu, Y., Fu, K., Bao, H., Song, D.: Development of a low-cost paper-based ELISA method for rapid *Escherichia coli* O157: H7 detection. Anal. Biochem. **542**, 58–62 (2018)
48. Feng, M., Yong, Q., Wang, W., Kuang, H., Wang, L., Xu, C.: Development of a monoclonal antibody-based ELISA to detect *Escherichia coli* O157: H7. Food Agric. Immunol. **24**, 481–487 (2013)
49. Jaria, G., Calisto, V., Otero, M., Esteves, V.I.: Monitoring pharmaceuticals in the aquatic environment using enzyme-linked immunosorbent assay (ELISA)—a practical overview. Anal. Bioanal. Chem. **412**, 3983–4008 (2020)
50. Černoch, I., Fránek, M., Diblíková, I., Hilscherová, K., Randák, T., Ocelka, T., Bláha, L.: Determination of atrazine in surface waters by combination of POCIS passive sampling and ELISA detection. J. Environ. Monit. **13**, 2582–2587 (2011)
51. Stephan, O., Vieths, S.: Development of a real-time PCR and a sandwich ELISA for detection of potentially allergenic trace amounts of peanut (*Arachis hypogaea*) in processed foods. J. Agric. Food Chem. **52**, 3754–3760 (2004)
52. Abbott, M., Hayward, S., Ross, W., Godefroy, S.B., Ulberth, F., Van Hengel, A.J., Roberts, J., Akiyama, H., Popping, B., Yeung, J.M.: Validation procedures for quantitative food allergen ELISA methods: community guidance and best practices. J. AOAC Int. **93**, 442–450 (2010)
53. Petrakova, A., Urusov, A., Zherdev, A., Dzantiev, B.: Magnetic ELISA of aflatoxin B1–pre-concentration without elution. Anal. Methods **7**, 10177–10184 (2015)

54. Urusov, A.E., Petrakova, A.V., Vozniak, M.V., Zherdev, A.V., Dzantiev, B.B.: Rapid immunoenzyme assay of aflatoxin B1 using magnetic nanoparticles. Sensors **14**, 21843–21857 (2014)
55. Gao, L., Zhuang, J., Nie, L., Zhang, J., Zhang, Y., Gu, N., Wang, T., Feng, J., Yang, D., Perrett, S.: Intrinsic peroxidase-like activity of ferromagnetic nanoparticles. Nat. Nanotechnol. **2**, 577–583 (2007)
56. Yang, M., Guan, Y., Yang, Y., Xia, T., Xiong, W., Wang, N., Guo, C.: Peroxidase-like activity of amino-functionalized magnetic nanoparticles and their applications in immunoassay. J. Colloid Interface Sci. **405**, 291–295 (2013)
57. Woo, M.-A., Kim, M.I., Jung, J.H., Park, K.S., Seo, T.S., Park, H.G.: A novel colorimetric immunoassay utilizing the peroxidase mimicking activity of magnetic nanoparticles. Int. J. Mol. Sci. **14**, 9999–10014 (2013)
58. Fu, G., Sanjay, S.T., Zhou, W., Brekken, R.A., Kirken, R.A., Li, X.: Exploration of nanoparticle-mediated photothermal effect of TMB-H_2O_2 colorimetric system and its application in a visual quantitative photothermal immunoassay. Anal. Chem. **90**, 5930–5937 (2018)
59. Le, T.N., Tran, T.D., Kim, M.I.: A convenient colorimetric bacteria detection method utilizing chitosan-coated magnetic nanoparticles. Nanomaterials **10**, 92 (2020)
60. Yang, W., Li, J., Wang, M., Sun, X., Liu, Y., Yang, J., Ng, D.H.: A colorimetric strategy for ascorbic acid sensing based on the peroxidase-like activity of core-shell Fe_3O_4/CoFe-LDH hybrid. Colloids Surf. B **188**, 110742 (2020)
61. Park, K.S., Kim, M.I., Cho, D.Y., Park, H.G.: Label-free colorimetric detection of nucleic acids based on target-induced shielding against the peroxidase-mimicking activity of magnetic nanoparticles. Small **7**, 1521–1525 (2011)
62. Kim, M.I., Shim, J., Parab, H.J., Shin, S.C., Lee, J., Park, H.G.: A convenient alcohol sensor using one-pot nanocomposite entrapping alcohol oxidase and magnetic nanoparticles as peroxidase mimetics. J. Nanosci. Nanotechnol. **12**, 5914–5919 (2012)
63. Baldrich, E., Muñoz, F.X.: Enzyme shadowing: using antibody–enzyme dually-labeled magnetic particles for fast bacterial detection. Analyst **133**, 1009–1012 (2008)
64. Li, J., Lillehoj, P.B.: Ultrafast electrothermal flow-enhanced magneto biosensor for highly sensitive protein detection in whole blood. Angew. Chem. e202200206 (2022) (online version)
65. Kim, S.U., Jo, E.-J., Mun, H., Noh, Y., Kim, M.-G.: Ultrasensitive detection of *Escherichia coli* O157: H7 by immunomagnetic separation and selective filtration with nitroblue tetrazolium/5-bromo-4-chloro-3-indolyl phosphate signal amplification. J. Agric. Food Chem. **66**, 4941–4947 (2018)
66. Sung, Y.J., Suk, H.-J., Sung, H.Y., Li, T., Poo, H., Kim, M.-G.: Novel antibody/gold nanoparticle/magnetic nanoparticle nanocomposites for immunomagnetic separation and rapid colorimetric detection of Staphylococcus aureus in milk. Biosens. Bioelectron. **43**, 432–439 (2013)
67. Yin, H.-Y., Li, Y.-T., Tsai, W.-C., Dai, H.-Y., Wen, H.-W.: An immunochromatographic assay utilizing magnetic nanoparticles to detect major peanut allergen Ara h 1 in processed foods. Food Chem. **375**, 131844 (2021)
68. Urusov, A.E., Petrakova, A.V., Zherdev, A.V., Dzantiev, B.B.: "Multistage in one touch" design with a universal labelling conjugate for high-sensitive lateral flow immunoassays. Biosens. Bioelectron. **86**, 575–579 (2016)
69. Tsai, T.-T., Huang, T.-H., Chen, C.-A., Ho, N.Y.-J., Chou, Y.-J., Chen, C.-F.: Development a stacking pad design for enhancing the sensitivity of lateral flow immunoassay. Sci. Rep. **8**, 1–10 (2018)
70. Tomás, A.L., De Almeida, M.P., Cardoso, F., Pinto, M., Pereira, E., Franco, R., Matos, O.: Development of a gold nanoparticle-based lateral-flow immunoassay for Pneumocystis pneumonia serological diagnosis at point-of-care. Front. Microbiol. **10**, 2917 (2019)
71. Zhang, J., Weng, Z., Du, H., Xu, F., He, S., He, D., Cheng, T., Zhang, J., Ge, S., Xia, N.: Development and evaluation of rapid point-of-care tests for detection of Enterovirus 71 and Coxsackievirus A16 specific immunoglublin M antibodies. J. Virol. Methods **231**, 44–47 (2016)
72. Qu, H., Zhang, Y., Qu, B., Kong, H., Qin, G., Liu, S., Cheng, J., Wang, Q., Zhao, Y.: Rapid lateral-flow immunoassay for the quantum dot-based detection of puerarin. Biosens. Bioelectron. **81**, 358–362 (2016)
73. Liang, Z.-Y., Deng, Y.-Q., Tao, Z.-Z.: A quantum dot-based lateral flow immunoassay for the rapid, quantitative, and sensitive detection of specific IgE for mite allergens in sera from patients with allergic rhinitis. Anal. Bioanal. Chem. **412**, 1785–1794 (2020)
74. Xia, X., Xu, Y., Zhao, X., Li, Q.: Lateral flow immunoassay using europium chelate-loaded silica nanoparticles as labels. Clin. Chem. **55**, 179–182 (2009)
75. Bamrungsap, S., Apiwat, C., Chantima, W., Dharakul, T., Wiriyachaiporn, N.: Rapid and sensitive lateral flow immunoassay for influenza antigen using fluorescently-doped silica nanoparticles. Microchim. Acta **181**, 223–230 (2014)
76. Liu, F., Zhang, H., Wu, Z., Dong, H., Zhou, L., Yang, D., Ge, Y., Jia, C., Liu, H., Jin, Q.: Highly sensitive and selective lateral flow immunoassay based on magnetic nanoparticles for quantitative detection of carcinoembryonic antigen. Talanta **161**, 205–210 (2016)
77. Zheng, C., Wang, X., Lu, Y., Liu, Y.: Rapid detection of fish major allergen parvalbumin using superparamagnetic nanoparticle-based lateral flow immunoassay. Food Control **26**, 446–452 (2012)
78. Razo, S.C., Panferov, V.G., Safenkova, I.V., Varitsev, Y.A., Zherdev, A.V., Dzantiev, B.B.: Double-enhanced lateral flow immunoassay for potato virus X based on a combination of magnetic and gold nanoparticles. Abal. Chim. Acta **1007**, 50–60 (2018)
79. Petrakova, A.V., Urusov, A.E., Zherdev, A.V., Dzantiev, B.B.: Immunochromatographic tests for mycotoxins detection with the use of ultrasmall magnetite nanoparticles. Eng. Proc. **2**, 100 (2020)
80. WHO Coronavirus (COVID-19) Dashboard. https://covid19.who.int/. Accessed 7 March 2022
81. Wu, K., Saha, R., Su, D., Krishna, V. D., Liu, J., Cheeran, M. C., Wang, J.-P.: Magnetic immunoassays: a review of virus and pathogen detection before and amidst the coronavirus disease-19 (COVID-19). arXiv preprint arXiv:2007.04809 (2020)
82. Petherick, A.: Developing antibody tests for SARS-CoV-2. Lancet **395**, 1101–1102 (2020)
83. Zhang, W., Du, R.-H., Li, B., Zheng, X.-S., Yang, X.-L., Hu, B., Wang, Y.-Y., Xiao, G.-F., Yan, B., Shi, Z.-L.: Molecular and serological investigation of 2019-nCoV infected patients: implication of multiple shedding routes. Emerg. Microbes Infect. **9**, 386–389 (2020)
84. Guo, L., Ren, L., Yang, S., Xiao, M., Chang, D., Yang, F., Dela Cruz, C.S., Wang, Y., Wu, C., Xiao, Y.: Profiling early humoral response to diagnose novel coronavirus disease (COVID-19). Clin. Infect. Dis. **71**, 778–785 (2020)
85. Liu, W., Liu, L., Kou, G., Zheng, Y., Ding, Y., Ni, W., Wang, Q., Tan, L., Wu, W., Tang, S.: Evaluation of nucleocapsid and spike protein-based enzyme-linked immunosorbent assays for detecting antibodies against SARS-CoV-2. J. Clin. Microbiol. **58**, e00461-00420 (2020)
86. Li, Z., Yi, Y., Luo, X., Xiong, N., Liu, Y., Li, S., Sun, R., Wang, Y., Hu, B., Chen, W.: Development and clinical application of a rapid IgM-IgG combined antibody test for SARS-CoV-2 infection diagnosis. J. Med. Virol. **92**, 1518–1524 (2020)

87. Soleimani, R., Khourssaji, M., Gruson, D., Rodriguez-Villalobos, H., Berghmans, M., Belkhir, L., Yombi, J.C., Kabamba-Mukadi, B.: Clinical usefulness of fully automated chemiluminescent immunoassay for quantitative antibody measurements in COVID-19 patients. J. Med. Virol. **93**, 1465–1477 (2021)
88. Chen, P.-Y., Ko, C.-H., Wang, C.J., Chen, C.-W., Chiu, W.-H., Hong, C., Cheng, H.-M., Wang, I.-J.: The early detection of immunoglobulins via optical-based lateral flow immunoassay platform in COVID-19 pandemic. PLoS ONE **16**, e0254486 (2021)
89. Huergo, L.F., Selim, K.A., Conzentino, M.S., Gerhardt, E.C., Santos, A.R., Wagner, B., Alford, J.T., Deobald, N., Pedrosa, F.O., De Souza, E.M.: Magnetic bead-based immunoassay allows rapid, inexpensive, and quantitative detection of human SARS-CoV-2 antibodies. ACS Sens. **6**, 703–708 (2021)
90. Sharma, M.K., Rao, V.K., Agarwal, G.S., Rai, G.P., Gopalan, N., Prakash, S., Sharma, S., Vijayaraghavan, R.: Highly sensitive amperometric immunosensor for detection of *Plasmodium falciparum* histidine-rich protein 2 in serum of humans with malaria: comparison with a commercial kit. J. Clin. Microbiol. **46**, 3759–3765 (2008)
91. Liu, D., Wang, Z., Jin, A., Huang, X., Sun, X., Wang, F., Yan, Q., Ge, S., Xia, N., Niu, G.: Acetylcholinesterase-catalyzed hydrolysis allows ultrasensitive detection of pathogens with the naked eye. Angew. Chem. **125**, 14315–14319 (2013)
92. Wang, J.-J., Jiang, Y.-Z., Lin, Y., Wen, L., Lv, C., Zhang, Z.-L., Chen, G., Pang, D.-W.: Simultaneous point-of-care detection of enterovirus 71 and coxsackievirus B3. Anal. Chem. **87**, 11105–11112 (2015)
93. Obst, U., Hubner, I., Wecker, M., Bitter-Suermann, D.: Immunological method using monoclonal antibodies to detect Enterobacteriaceae in drinking water. Aqua **38**, 136–142 (1989)
94. Holzhauser, T., Johnson, P., Hindley, J.P., O'Connor, G., Chan, C.-H., Costa, J., Fæste, C.K., Hirst, B.J., Lambertini, F., Miani, M.: Are current analytical methods suitable to verify VITAL® 2.0/3.0 allergen reference doses for EU allergens in foods? Food Chem. Toxicol. **145**, 111709 (2020)
95. Liu, Q., Tang, P., Xing, X., Cheng, W., Liu, S., Lu, X., Zhong, L.: Colorimetry/SERS dual-sensor of H_2O_2 constructed via TMB–Fe_3O_4@ AuNPs. Talanta **240**, 123118 (2021)
96. Zhang, X., Rao, H., Huang, H., Zhang, K., Wei, M., Luo, M., Xue, X., Xue, Z., Lu, X.: A sensitive photothermometric biosensor based on redox reaction-controlled nanoprobe conversion from Prussian blue to Prussian white. Anal. Bioanal. Chem. **413**, 6627–6637 (2021)